IEEE Access
Multidisciplinary ⋮ Rapid Review ⋮ Open Access Journal

Received July 19, 2020, accepted August 2, 2020, date of publication August 10, 2020, date of current version August 21, 2020.

Digital Object Identifier 10.1109/ACCESS.2020.3015487

A Novel Dynamic Spectrum-Sharing Method for GEO and LEO Satellite Networks

YUNFENG WANG[1], XIAOJIN DING[1,2], (Member, IEEE), AND GENGXIN ZHANG[1], (Member, IEEE)

[1]Key Laboratory of Broadband Wireless Communication and Sensor Network Technology, Nanjing University of Posts and Telecommunications (NUPT), Nanjing 210003, China
[2]National Mobile Communications Research Laboratory, Southeast University, Nanjing 210096, China

Corresponding author: Xiaojin Ding (dxj@njupt.edu.cn)

This work was supported in part by the National Science Foundation of China under Grant 91738201 and Grant 61772287, in part by the China Postdoctoral Science Foundation under Grant 2018M632347, in part by the Natural Science Foundation for Jiangsu Higher Education Institutions under Grant 18KJB510030 and Grant 16KJB510031, in part by the Key University Science Research Project of Jiangsu Province under Grant 18KJA510004, and in part by the Postgraduate Research and Practice Innovation Program of Jiangsu Province under Grant KYCX20_0708.

ABSTRACT In this article, we investigate the spectrum-sharing for a space information network comprised of a geostationary orbit (GEO) satellite and a pair of low earth orbit (LEO) satellites, where one spectrum-sensing LEO (SLEO) is used to sense the status of spectrum occupancy of the GEO, and one data-transmission LEO (DLEO) satellite is allowed to access the shared spectrum of the GEO with the aid of the SLEO. In order to improve the throughput of the DLEO satellite, a spectrum sharing framework has been conceived relying on two stages. Differing from the conventional spectrum-sharing scheme, the data-transmission LEO satellite has the ability to access the shared spectrum both in overlay mode and in underlay mode. In overlay mode, the DLEO can perform transmission at any required transmit power. By contrast, in underlay mode, a spectrum-sensing and power allocation aided spectrum-sharing (SPA-SS) scheme is proposed to guarantee that the maximal amount of interference is imposed on the GEO caused by the DLEO. To be specific, in the first stage, the SLEO is invoked for performing spectrum-sensing, where the time intervals of spectrum-sensing have been specifically optimized to alleviate the interference received at the GEO in the second stage. Moreover, an adaptive power allocation is designed to maximal the throughput of the DLEO in the second stage, whilst maintaining the maximal interference imposed on the GEO is lower than the tolerable interference temperature of the GEO. Numerical results show that the proposed SPA-SS scheme outperforms the traditional spectrum-sharing scheme in terms of not only the average throughput, but also of the time-utilization ratio.

INDEX TERMS Cognitive satellite network, spectrum coexistence, spectrum sensing, Hidden Markov model, sensing time interval.

I. INTRODUCTION

With the increasing number of LEO satellites in the space, the available radio spectrum resource is scarce, which is a bottleneck for the satellite system development. Therefore, the next generation satellite system require significantly high spectral efficiency to address the spectrum scarcity problem between GEO system and LEO system. In order to achieve this objective, different satellite systems need to coexist within the same spectrum, which means that more interference may occur between these two satellite systems [1]–[3]. Recently, cognitive radio (CR) has received great attention as a promising solution to the inadequacy of spectrum [4]–[9]. In CR, with the aid of spectrum sensing, it enables the detection of under-utilized licensed frequency bands and the opportunistic use of such bands by the unlicensed users, thereby increasing the spectrum utilization [10]–[14].

In recent years, spectrum sensing for satellite communications has gained many accomplishments, which can be categorized into the contributions in [15]–[21] focus on hybrid coexistence scenario of satellite and terrestrial systems and the contributions in [22]–[28] address dual satellite coexistence scenarios. However, the interference in the satellite system is different from that of the terrestrial systems, which is mainly caused by the sidelobes in the on-board antenna radiation diagram i.e., non-ideal angular selectivity of the spotbeams [29]. Furthermore, the system

The associate editor coordinating the review of this manuscript and approving it for publication was Haipeng Yao.

architecture will dynamically change for LEO satellites. If an LEO system coexists with another satellite system, it is very likely to produce in-line interference when the satellites and users from different systems are in alignment, which will make the systems paralyzed. Therefore, it is of great importance to analyze the co-frequency interference between LEO and GEO systems.

To address the challenge, there are many researches objecting at the in-line interference in the published paper. Reference [30] studies the coexistence downlink interference between LEO system and GEO system and evaluates the impact of the exclusive angel strategy on the inference. The feasibility of spectrum sharing between GEO and Non-geostationary orbit (NGSO) satellite systems through a database approach is analyzed in [31]. Meanwhile, reference [26] utilized the adaptive power control (APC) to mitigate the in-line interference between the GEO and NGSO systems. Reference [25] proposed a cognitive broadband satellite network based on the beam hopping and APC techniques. In addition, reference [32] analyzes the interference caused by terrestrial cellular systems and NGSO systems to GEO systems, respectively, and calculates the protection area where no cognitive users (terrestrial system or NGSO system) could transmit.

Remarkably, the aforementioned works were based on the assumption that all the LEO satellites have sensing functions. However, this is not in line with the actual situation. In practice, most of LEO satellites in space are not equipped with sensing satellite payloads due to the weight, space and other constraints. In this article, we propose a general framework, which is fit for spectrum sensing and satellite data transmission. In this framework, with the help of a cognitive satellite, the LEO satellite that has no sensing function but needs data transmission can share spectrum with GEO satellite. Specifically, the GEO system is regarded as a primary user, the LEO system needs to transmit date is denoted as a secondary user, while another cognitive satellite can be regarded as a sensing payload separate from the LEO system.

Furthermore, traditional spectrum sensing methods require that a secondary user sense the spectrum at the beginning of each time slot. However, in some practical satellite scenarios, the access pattern of the GEO system can be characterized by a statistical model, the future status of the GEO system can be predicted to some extent [33]–[40]. Based on this observation, the LEO satellites is unnecessarily to sense the channel at the beginning of each time slot. In particular, the total in-line interference time of GEO and LEO system is often a constant; a more frequent sensing will waste of data transmission time, which leads to smaller throughput. On the other hand, the fewer often sensing may miss some transmission opportunities when the current channel status of GEO system is busy, or incur some transmission collisions when the current channel status is idle. Therefore, the spectrum sensing interval must be carefully investigated, which has already been studied in [37]. However, the spectrum sensing interval was optimized at different spectrum sensing results in [37], but in this article, we extend this problem to satellite communication scenario, and investigate algorithm that jointly optimize the spectrum sensing time, the spectrum sensing interval and the LEO system transmit power to enhance spectral efficiency and ensure the coexistence without disruption.

In this article, we propose a general framework, where the LEO system has the ability to work concurrently with GEO systems in the interference region. Noted that LEO system will also stop working to protect the GEO system when the interference is very serious. Our contributions in this article can be summarized as follows.

1) By jointly considering the advantage of spectrum-sensing and power control, a two-stage aided spectrum-sharing framework is conceived. Specifically, differing from conventional spectrum-sharing scheme, the data transmission LEO (DLEO) is allowed to access the shared the spectrum of the GEO in both overlay mode and in underlay mode, in order to maximize the average throughput.
2) We propose a spectrum-sensing and power allocation aided spectrum-sharing (SPA-SS) scheme. To be specific, the proposed SPA-SS scheme can guarantee that the maximal amount of interference is imposed on the GEO caused by the DLEO, relying on the optimized time intervals of spectrum-sensing and transmit power of the DLEO.
3) Numerical results show that compared the conventional spectrum-sharing scheme, the proposed SPA-SS scheme can not only achieve higher average throughput, but also attain better time-utilization ratio, showing the advantage of the propose SPA-SS scheme.

The remainder of this article is organized as follows: In Section II presents the interference analysis model, sensing analysis model and the GEO activity mode, respectively. Section III, the joint optimization of spectrum sensing time, sensing interval and DLEO system transmit power is proposed to maximize the average throughput of DLEO system, and the two-dimensional line search method and the KKT (Karush-Kuhn-Tucker) conditions are used to solve the problem. In Section IV, the simulation results are presented to evaluate the designed algorithm. Finally, some conclusions are drawn in Section V.

II. SYSTEM MODEL

A. SATELLITE NETWORK MODLE

We consider the spectrum sharing between the LEO and GEO system model. The GEO system, as the primary user, has the priority to use the frequency. The LEO satellite acts as the secondary system, which should coordinate to avoid disrupting the incumbent GEO system. As described in Fig.1, the spectrum-sensing LEO (SLEO) is used to sense the status of spectrum occupancy of the GEO, and the data-transmission LEO (DLEO) satellite is allowed to access the shared spectrum of the GEO with the aid of the SLEO. Furthermore, in this cognitive satellite network, it is assumed that the earth

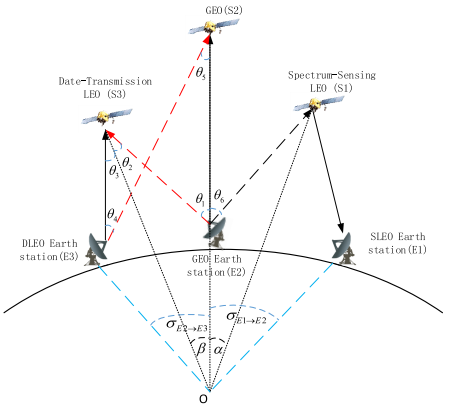

FIGURE 1. Spectrum coexistence between the GEO and LEO system.

stations of three systems are connected by a high-speed lossless fiber optic connection and exchange satellite ephemeris with each other.

1) MODEL ANALYSIS

Based on the previous analysis, we propose a spectrum-sharing scenario between GEO and LEO system. As shown in Fig.1, the model consists of a DLEO satellite and its earth station, which is recorded as S3 and E3 respectively, a GEO satellite and its earth station, which is recorded as S2 and E2 respectively, a SLEO satellite and its earth station, which is recorder as S1 and E1 respectively. Without loss of generality, the S2 and its earth station E2 are located in the same line with the origin of the earth. In addition, the relative positions of E1, E2 and E3 are also crucial factors in the interference analysis. Let $\sigma_{E1\to E2}$,$\sigma_{E2\to E3}$ denote the geocentric angle between E1 and E2, E2 and E3, respectively. Yet the general, these two angles can be regarded as constants in next interference analysis. Furthermore, $\{d_{Ei\to Ej}|i \in (1,2,3), j \in (1,2,3), i \neq j\}$, represents the distance between the E_i and E_j, and $\{d_{Si\to Sj}|i \in (1,2,3), j \in (1,2,3), i \neq j\}$, represents the distance between the S_i and S_j, and $\{d_{Ei\to Sj}|i \in (1,2,3), j \in (1,2,3)\}$, represents the distance between the E_i and S_j. As shown in the Fig.1, θ_1-θ_6 is the off-axis angle of the $E2$ towards to $S3$, the $S3$ towards to the $E2$, the $S3$ towards to $E3$, the $E3$ towards to the $S2$, the $S2$ towards to $E3$, the $E2$ towards to $S1$, respectively. Let β denotes the geocentric angle between the S_2 and S_3, Let α denotes the geocentric angle between the S_1 and S_2. It is obvious that the α, β changes with the LEO satellite moving. In addition, the distance $d_{S3\to E2}$, $d_{S3\to S2}$, $d_{S3\to E3}$ is the function of β, and the distance $d_{S1\to E2}$, $d_{S1\to S2}$ is the function of α, they can be rewritten as

$$d_{S3\to E2} = \sqrt{d_{S3}^2 + R^2 - 2Rd_{S3}\cos\beta} \tag{1}$$

$$d_{S3\to E3} = \sqrt{d_{S3}^2 + R^2 - 2Rd_{S3}\cos(\sigma_{E2\to E3} - \beta)} \tag{2}$$

$$d_{S3\to S2} = \sqrt{d_{S3}^2 + d_{S2}^2 - 2d_{S2}d_{S3}\cos\beta} \tag{3}$$

$$d_{S1\to E2} = \sqrt{d_{S1}^2 + R^2 - 2Rd_{S1}\cos\alpha} \tag{4}$$

$$d_{S1\to S2} = \sqrt{d_{S1}^2 + d_{S2}^2 - 2d_{S1}d_{S2}\cos\alpha} \tag{5}$$

where R denotes the radius of the earth, d_{S1}, d_{S2}, d_{S3} denote the distance between the $S1\backslash S2\backslash S3$ and the center of the earth, respectively. In addition, the angles θ_1-θ_6 can be derived as follows

$$\theta_1 = \arccos\left(\frac{(d_{S3\to E2})^2 + (d_{S2} - R)^2 - (d_{S3\to S2})^2}{2d_{S3\to E2}(d_{S2} - R)}\right) \tag{6}$$

$$\theta_2 = \arccos\left(\frac{(d_{S3\to E3})^2 + (d_{S3\to E2})^2 - (R\sigma_{E2\to E3})^2}{2d_{S3\to E3}d_{S3\to E2}}\right) \tag{7}$$

$$\theta_3 = \arccos\left(\frac{(d_{S3\to E3})^2 + (d_{S3})^2 - (R)^2}{2d_{S3\to E3}d_{S3}}\right) \tag{8}$$

$$\theta_4 = \arccos\left(\frac{(d_{S3\to E3})^2 + (d_{S2\to E3})^2 - (d_{S2\to S3})^2}{2d_{S3\to E3}d_{S2\to E3}}\right) \tag{9}$$

$$\theta_5 = \arccos\left(\frac{(d_{S2\to E3})^2 + (d_{S2})^2 - (R)^2}{2d_{S2\to E3}d_{S2}}\right) \tag{10}$$

$$\theta_6 = \arccos\left(\frac{(d_{S2} - R)^2 + (d_{S1\to E2})^2 - (d_{S1\to})^2}{2(d_{S2} - R)d_{S1\to S2}}\right) \tag{11}$$

where $d_{S2\to E3} = \sqrt{R^2 + d_{S2}^2 - 2Rd_{S2}\cos\sigma_{E2\to E3}}$

2) INTERFERENCE ANALYSIS

Note that in this article, we focus on the interference both experienced by the DLEO and GEO satellite system. As described in Fig.1, the GEO earth station and GEO satellite would be interfered by the DLEO satellite in the downlink and the DLEO earth station in the uplink, respectively. Meanwhile, the DLEO earth station and DLEO satellite would be also interfered by the GEO system. However, the analysis method of the interference in the downlink is similar to that in the uplink. In this article, we only analyze the interference in uplink scenario.

The DLEO earth station transmits the signal to its satellite, and the power of the received signal at DLEO satellite can be expressed as

$$\begin{aligned} P_{S3} &= P_{E3}h_{E3\to S3} \\ &= P_{E3}G_{E3}^t G_{E3}^r(\theta_3)\left(\frac{c}{4\pi f d_{E3\to S3}}\right)^2 \end{aligned} \tag{12}$$

with P_{S3} as the transmission power at DLEO station, G_{E3}^t as the maximum gain of LEO earth station transmit antenna, $G_{E3}^r(\theta_3)$ as the gain of the DLEO receive antenna to the direction of its satellite, c as the light speed, and f as the center frequency of the spectrum bands. Note that the antenna gain is related to the off-boresight angle of the transmitter or receiver in the beam direction, the off-boresight angle can be calculated through the beam direction and the position vector of the satellite and user [41]. Note that the angle θ varies when the satellite moves, which results in the dynamic of the gain. The expression to calculate the gain of the antenna is [42]

$$G = G_0\left(\frac{J_1(\mu)}{2\mu} + 36\frac{J_3(\mu)}{\mu^3}\right) \tag{13}$$

where $\mu = 2.07123\sin(\theta)/\sin(\theta_{3dB})$, J_1 and J_3 are the first and third order Bessel functions, respectively. θ is the off boresight angle, θ_{3dB} is the angle that corresponds to the 3dB

Beamwidth, G_0 is the maximum antenna gain when the off boresight angle is 0, and its expression is

$$G_0 = \eta \frac{4\pi A}{(c/f)^2} \tag{14}$$

where A represents the antenna area, η represents the antenna efficiency. Meanwhile, the DLEO may receive the signal from GEO earth station, thus the interference from the GEO earth station to the DLEO satellite can be expressed as

$$I_{S3} = P_{E2} G^t_{E2\to S3}(\theta_1) G^r_{S3\to E2}(\theta_2) \left(\frac{c}{4\pi f d_{S3\to E2}} \right)^2 \tag{15}$$

with P_{E2} as the transmission power at GEO station, $G^t_{E2\to S3}$ as the gain of the GEO earth station transmit antenna to the direction of the DLEO satellite, $G^r_{S3\to E2}(\theta_2)$ as the gain of the DLEO receive antenna to the direction of the GEO earth station.

From the equations above, it can be found that both the signal power and the interference are related to the angle β. Thus, we can conclude that the received Signal Noise Ratio (SNR) is also the function of angle β, which can be expressed as follows

$$\begin{aligned} \gamma_{S3} &= \frac{P_{S3}}{I_{S3} + N_0} = \frac{P_{S3}(\beta)}{I_{S3}(\beta) + N_0} \\ N_0 &= kT_nB \end{aligned} \tag{16}$$

where k is Boltzmann constant, T_n represents the equivalent noise temperature of the receiver, and B represents the transponder bandwidth. The GEO receives the signal from the GEO earth station, meanwhile, it also may receive the signal from DLEO earth station. The analytical method in GEO system is similar to that in the DLEO system, the power of the received signal at LEO can be expressed as

$$\begin{aligned} P_{S2} &= P_{E2} h_{E2\to S2} \\ &= P_{E2} G^t_{S2} G^r_{S2} \left(\frac{c}{4\pi f (d_{S2} - R)} \right)^2 \end{aligned} \tag{17}$$

with P_{E2} as the transmission power at GEO earth station, G^t_{S2} as the maximum gain of GEO earth station transmit antenna, G^r_{S2} as the gain of the maximum gain of GEO receive antenna. The interference from the LEO earth station to the GEO satellite can be expressed as

$$I_{S2} = P_{E3} G^t_{E3\to S2}(\theta_4) G^r_{S2\to E3}(\theta_5) \left(\frac{c}{4\pi f d_{S2\to E3}} \right)^2 \tag{18}$$

with P_{E3} as the transmission power at DLEO station, $G^t_{E3\to S2}(\theta_4)$ as the gain of the DLEO earth station transmit antenna to the direction of the GEO, $G^r_{S2\to E3}(\theta_5)$ as the gain of the GEO receive antenna to the direction of the DLEO earth station. Thus, we can conclude that the received SNR of GEO is also the function of angle β, which can be expressed as follows

$$\gamma_{S2} = \frac{P_{S2}}{I_{S2} + N_0} = \frac{P_{S2}(\beta)}{I_{S2}(\beta) + N_0} \tag{19}$$

The satellite orbital parameters and system parameters are presented in Table.4 and Table.5. Based on the previous analysis, the received SNR of DLEO satellite and that of

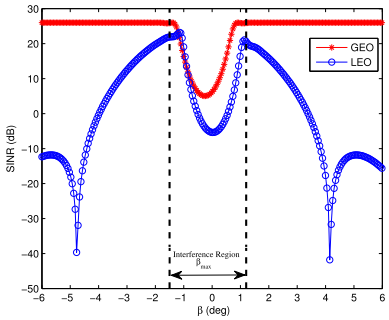

FIGURE 2. Received SNR by LEO and GEO satellite with respect to varying β when $\sigma_{E2\to E3} = -0.3^o$.

GEO satellite varies with angle β, as described in Fig.2. Furthermore, it can be seen that the SNR of the LEO and GEO is stability except of some regions where the SNR level is significantly low. We define the value of β_{max} corresponding to the dropped portion as interference region.

The received SNR of the DLEO and GEO satellites varies dramatically only when the DLEO satellite moves to the interference regions. It means that when the DLEO satellite enters into the interference region, it cannot transmit signals at will so as not to interfere to GEO system. Thus, we conceive a spectrum-sharing framework relying on two stages to improve the throughput of the DLEO satellite, where the DLEO satellite has the ability to access the shared spectrum with the aid of the SLEO. To be specific, in the first stage, the SLEO is invoked for perform spectrum-sensing to detect the spectrum hole of the GEO system, and the DLEO satellite can access the shared spectrum both in overlay mode and in underlay mode in the second state.

3) COGNITIVE SATELLITE ANALYSIS

In this section, we analyze the spectrum sensing of the SLEO in the first state. When the DLEO moves to the interference regions, DLEO earth station will send request information to SLEO system for spectrum sensing through ground optical fiber system before transmitting signal. Then according to the sensing results returned by the SLEO system, the DLEO system selects the shared spectrum access mode. Specifically, The GEO signal received by the SLEO can be written as

$$y_{S1} = \begin{cases} \sqrt{P_{E2}}\sqrt{h_{E2\to S1}} S_{E2} + N_0, & H_1 \\ N_0, & H_0 \end{cases} \tag{20}$$

$$h_{E2\to S1} = G^t_{E2\to S1}(\theta_6) G^r_{S1} \left(\frac{c}{4\pi f d_{S1\to E2}} \right)^2 \tag{21}$$

with $G^t_{E2\to S1}(\theta_6)$ as the gain of the GEO earth station to the direction of SLEO satellite, G^r_{S1} as the maximum gain of SLEO receive antenna. In addition, H_0 represents the hypothesis that the GEO system is absent; H_1 denotes the hypothesis that the GEO system operates. Thus, the receive SNR of SLEO can be expressed as

$$\begin{aligned} \gamma_{S1} &= \frac{P_{E2} h_{E2\to S1}}{N_0} \\ &= \frac{P_{E2} G^r_{S1} G^t_{E2\to S1}(\theta_6) \left(\frac{c}{4\pi f d_{S1\to E2}} \right)^2}{kT_nB} \end{aligned} \tag{22}$$

Apparently, the received SNR is the function of angle α and varies with α. Furthermore, we can derive the detection probability and false alarm probability as follows[11]

$$Pd_{S1} = Q\left(\left(\frac{\varepsilon}{N_0} - \gamma_{S1} - 1\right)\sqrt{\frac{T_s f_s}{2\gamma_{S1}+1}}\right) \tag{23}$$

$$Pf_{S1} = Q\left(\left(\frac{\varepsilon}{N_0} - 1\right)\sqrt{T_s f_s}\right) \tag{24}$$

where ε stands for detection threshold, T_s is the sensing time, and f_s is the sampling frequency of the SLEO. Obviously, the detection probability and false alarm probability are the function of angle α and sensing time T_s.

4) GEO SYSTEM ACTIVITY MODEL

We model the GEO system states as a two-state on-off Markov chain, which has been widely used in terrestrial CR networks. Compared with the ground network, the satellite system modeling as Hidden Markov Model (HMM) has more advantages. The SLEO system can obtain the training sequence through repeated visits to GEO's coverage area without its any prior knowledge due to that the satellite channel can be regarded as AWGN channel, where the channel gain is fixed. Since the estimation accuracy of the GEO's parameters depends on the length of the training sequence, for simplicity, the following analysis assumes that the error of estimation can be ignored. Thus, the transition matrix of HMM is denoted by

$$\Delta_{S2} = \begin{bmatrix} \eta_{00} & \eta_{01} \\ \eta_{10} & \eta_{11} \end{bmatrix} \tag{25}$$

where $\eta_{ij} = Pr\{q_{t-1}^{S2} = H_j | q_t^{S2} = H_i\}, i, j = 0, 1$, q_t^{S2} is the state of the GEO system at slot t. Hence, given the transition matrix Δ_{S2} and the initial distribution of the states O_{S2}, we can calculate the probability that the state lasts for exactly ρ slots [37].

III. PROBLEM FORMULATION

A. SENSING INTERVAL ANALYSIS

In practices, the time that DLEO satellite pass through the interference region is a constant, which can be divided into the same time slot τ. Since the future state of the GEO system can be predicted to some extent, the interval Θ consisting of several time slots is a crucial factor in the throughput analysis. As described in Fig.3. Each interval is divided into three phases: the sensing phase T_s, the sensing result reporting phase T_t and the DLEO system transmission phase T_{LEO}, $T_{LEO} = \Theta\tau - T_s - T_t$. Obviously, a larger interval will reduce the number of sensing times, and the throughput will increase due to more time remained for data transmission. On the other hand, a larger interval may also miss some transmission opportunities when the GEO current channel status is busy, or incur some transmission collisions when the current channel status is idle. Thus, the spectrum sensing interval must be carefully studied to determine.

The activity of the GEO system is difficult to be precisely predicted, it may change its state during several consecutive slots. We solve this problem by studying the average

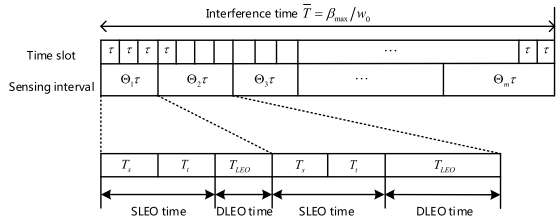

FIGURE 3. Time slot structure of the proposed spectrum-sharing algorithm in satellite networks.

free/busy time in an interval. Without loss of generality, let random variable X1 denotes the number of the busy slots during Θ consecutive slots. However, different channel statuses have different duration probability density functions. Therefore, we derive the mean of X1 independently for two cases: the initial channel status is busy or idle.

Case 1: the current true channel state is busy, the expectation of X1 can be rewritten as:

$$E\left(X_1^1\right) = \begin{cases} E\left(X_1^1\right)|^1, & \text{if b is odd} \\ E\left(X_1^1\right)|^0, & \text{if b is even} \end{cases} \tag{26}$$

where b is the number of state changes during Θ slots. Note that if b is odd, it means that the last channel state must be busy, if even, it means the last state must be idle. Thus, the expression of $E\left(X_1^1\right)$ is given by [37]

$$E\left(X_1^1\right)|^1 = \begin{cases} \sum_{b=0}^{\Theta-1} \sum_{m=\frac{b+1}{2}}^{\Theta-\frac{b+1}{2}} Pr_1\left(X_1 = m\right) m & \Theta > 1 \\ 1 & \Theta = 1 \end{cases} \tag{27}$$

where $Pr_1\left(X_1 = m\right) = C_{m-1}^{\frac{b-1}{2}} C_{\Theta-m-1}^{\frac{b-1}{2}} \left(\eta_{11}\right)^m \left(\eta_{00}\right)^{\Theta-m} \left(\frac{\eta_{10}\eta_{01}}{\eta_{11}\eta_{00}}\right)^{\frac{b+1}{2}} \left(\eta_{01}\right)^{-1}$, And the expression of $E\left(X_1^1\right)|^0$ is given by

$$E\left(X_1^1\right)|^0 = \begin{cases} \sum_{b=0}^{\Theta-1} \sum_{m=\frac{b}{2}+1}^{\Theta-\frac{b}{2}} Pr_2\left(X_1 = m\right) m & \Theta > 1 \\ 1 & \Theta = 1 \end{cases} \tag{28}$$

where $Pr_2\left(X_1 = m\right) = C_{m-1}^{\frac{b}{2}} C_{\Theta-m-1}^{\frac{b-2}{2}} \left(\eta_{11}\right)^m \left(\eta_{00}\right)^{\Theta-m} \left(\frac{\eta_{10}\eta_{01}}{\eta_{11}\eta_{00}}\right)^{\frac{b}{2}} \left(\eta_{11}\right)^{-1}$

Case 2: the current true channel state is idle, the expectation of X1 can be rewritten as:

$$E\left(X_1^0\right) = \begin{cases} E\left(X_1^0\right)|^1, & \text{if b is even} \\ E\left(X_1^0\right)|^0, & \text{if b is odd} \end{cases} \tag{29}$$

Note that if b is even, it means that the last channel state must be busy, if odd, it means the last state must be idle. Thus, the expression of $E\left(X_1^0\right)|^0$ is given by [37]

$$E\left(X_1^0\right)|^0 = \begin{cases} \sum_{b=0}^{\Theta-1} \sum_{m=\frac{b+1}{2}}^{\Theta-\frac{b+1}{2}} Pr_3\left(X_1 = m\right) m & \Theta > 1 \\ 0 & \Theta = 1 \end{cases} \tag{30}$$

TABLE 1. The GEO'S true channel state and sensing result, time allocation and related transmit power.

GEO state	Sening-result	Useful time		Interference time	Related Power
		Overlay	*Underlay*		
Idle: $P(H_0)$	Idle:$1-Pf_{S1}$	v_1	0	v_2	P^0_{E3}
Idle: $P(H_0)$	Busy:Pf_{S1}	v_1	v_2	0	P^1_{E3}
Busy: $P(H_1)$	Idle:$1-Pd_{S1}$	v_4	0	v_3	P^0_{E3}
Busy: $P(H_1)$	Busy:Pd_{S1}	v_3	v_4	0	P^1_{E3}

where $Pr_3(X_1=m)=C^{\frac{b-1}{2}}_{m-1}C^{\frac{b-1}{2}}_{\Theta-m-1}(\eta_{11})^m(\eta_{00})^{\Theta-m}$ $\left(\frac{\eta_{10}\eta_{01}}{\eta_{11}\eta_{00}}\right)^{\frac{b+1}{2}}(\eta_{10})^{-1}$, And the expression of $E(X^0_1)|^1$ is given by

$$E(X^0_1)|^1=\begin{cases}\sum_{b=0}^{\Theta-1}\sum_{m=\frac{b}{2}}^{\Theta-\frac{b+2}{2}}Pr_4(X_1=m)m & \Theta>1\\ 0 & \Theta=1\end{cases} \tag{31}$$

where $Pr_4(X_1=m)=C^{\frac{b-2}{2}}_{m-1}C^{\frac{b}{2}}_{\Theta-m-1}(\eta_{11})^m(\eta_{00})^{\Theta-m}$ $\left(\frac{\eta_{10}\eta_{01}}{\eta_{11}\eta_{00}}\right)^{\frac{b}{2}}(\eta_{00})^{-1}$.

B. OPTIMIZATION PROBLEM FORMULATION

In the interference region, the DLEO has the ability to access the shared-spectrum both in overlay mode and in underlay mode. Specifically, if the current true channel state during Θ consecutive slots is idle, the DLEO works in overlay mode and the transmit power is set to P^0_{E3}; if the current true channel state is busy, the DLEO works in underlay mode and the transmit power is set to P^1_{E3}, obviously, $P^0_{E3}\geq P^1_{E3}$. Furthermore, it is worth remarking that the active state of the GEO system may not maintain consecutive Θ slots and the true current state of the GEO system may be change. Thus, when the current sensing result is idle, using P^0_{E3} as the transmitting power may lead to some interference to the GEO system due to the current true channel state of GEO system has changed to busy. In addition, the imperfect characteristics of the spectrum sensing may also results in some interference. Therefore, the useful throughput of the DLEO system for the four different cases that listed in Table 1 are given as

$$C_{00}=\frac{1}{\Theta\tau}\left(v_1\log_2\left(1+\frac{P^0_{E3}}{N_0}\right)\right) \tag{32}$$

$$C_{01}=\frac{1}{\Theta\tau}\left(v_1\log_2\left(1+\frac{P^1_{E3}}{N_0}\right)+v_2\log_2\left(1+\frac{P^1_{E3}}{I_{S3}+N_0}\right)\right) \tag{33}$$

$$C_{10}=\frac{1}{\Theta\tau}\left(v_3\log_2\left(1+\frac{P^0_{E3}}{N_0}\right)\right) \tag{34}$$

$$C_{11}=\frac{1}{\Theta\tau}\left(v_3\log_2\left(1+\frac{P^1_{E3}}{I_{S3}+N_0}\right)+v_4\log_2\left(1+\frac{P^1_{E3}}{N_0}\right)\right) \tag{35}$$

where v_1, v_2, v_3 and v_4 are defined as

$$\begin{aligned}v_1&=T_{LEO}-E(X^0_1)\tau\\ v_2&=E(X^0_1)\tau\\ v_3&=E(X^1_1)\tau-T_s-T_t\\ v_4&=\Theta\tau-E(X^1_1)\tau\end{aligned} \tag{36}$$

The goal in this section is to maximize the throughput of DLEO system, while satisfying the corresponding constraints. From Table.1, the average throughput of the DLEO system per slot when the spectrum sensing interval is Θ are given as

$$\overline{C_{E3\to S3}}=U_{00}C_{00}+U_{01}C_{01}+U_{10}C_{10}+U_{11}C_{11} \tag{37}$$

where U_{00}, U_{01}, U_{10} and U_{11} represents the probability of four cases, respectively. Since $P(H_0)$ and $P(H_1)$ are the probabilities of idle status and busy status of the GEO system, they can be defined as

$$\begin{aligned}U_{00}&=P(H_0)(1-Pf_{S1})\\ U_{01}&=P(H_0)(Pf_{S1})\\ U_{10}&=P(H_1)(1-Pd_{S1})\\ U_{11}&=P(H_1)(Pd_{S1})\end{aligned} \tag{38}$$

And the average interference to the GEO system when the spectrum sensing interval is Θ is given as

$$\overline{I_{S2}}=\frac{1}{\Theta\tau}\left[\begin{pmatrix}U_{00}v_2P^0_{E3}+U_{01}v_2P^1_{E3}\\ +U_{10}v_3P^0_{E3}+U_{11}v_3P^1_{E3}\end{pmatrix}G_{S3}\{\beta\}\right] \tag{39}$$

where $G_{S3}\{\beta\}$ is defined as

$$G_{S3}\{\beta\}=G^t_{E3\to S2}(\theta_4)G^r_{S2\to E3}(\theta_5)\left(\frac{c}{4\pi fd_{S2\to E3}}\right)^2 \tag{40}$$

In addition, the sensing time T_s of the SLEO is also incorporated as an optimization variable. In particular, for a given target false-alarm probability $\overline{Pf_{S1}}$, the detection probability Pd_{S1} is calculated as [11]

$$Pd_{S1}=Q\left(\frac{1}{\sqrt{2\gamma_{s1}+1}}(Q^{-1}(\overline{Pf_{s1}})-\gamma_{s1}\sqrt{T_sf_s})\right) \tag{41}$$

which readily shows that a higher T_s leads to a lower Pf_{S1} and a higher Pd_{S1}, and thus improving the system performance. However, increasing T_s also decreases system throughout by reducing the time for the data transmission. Consequently, from Eq.23 and Eq.24, the constraint $T_{\min}$ is considered, where

$$T_{\min}=\frac{1}{(\gamma_{S1})^2f_s}\left[Q^{-1}(\overline{Pf_{S1}})-Q^{-1}(Pd_{S1})\sqrt{2\gamma_{S1}+1}\right]^2 \tag{42}$$

Furthermore, the maximum value of sensing interval $\Theta_{\max}$ is also limit. On the one hand, the larger $\Theta_{\max}$ will waste of the computing resources due to the active state of GEO system cannot stay the same for a long time. On the other hand, the DLEO satellite is moving at high speed, too large interval will lead to the dynamic change of SNR in this time slot, thus affecting the accuracy of the algorithm. Note that the proposed algorithm assumes the SNR does not change in

a sensing interval. Without loss of generality, we set $\Theta_{\max}$ as a small integer according to the GEO's state transition matrix and DLEO's high dynamicity.

In this article, we investigate to maximize the throughput of DLEO system by jointly deriving the transmitting power, sensing interval and sensing time under the minimum rate requirements for DLEO system, the transmit power constraints at the DLEO earth station, and the interference power constraints at the GEO system. In particular, the following optimization problem is given as:

$$\mathbf{P1}: \underset{P^0_{E3},P^1_{E3},\Theta,T_s}{\text{maximize}}\ \overline{C_{E3\to S3}} \tag{43}$$

$$\text{suject to C1:}\quad \overline{C_{E3\to S3}} \geq C^{\min}_{E3\to S3} \tag{43a}$$

$$\text{C2:}\quad 0 \leq P^i_{E3} \leq P^{\max}_{E3},\ i=0,1 \tag{43b}$$

$$\text{C3:}\quad 0 \leq \overline{I_{S2}} \leq I^{\max}_{S2} \tag{43c}$$

$$\text{C4:}\quad P^1_{E3}G_{S3}\{\beta\} \leq I^{\max}_{S2} \tag{43d}$$

$$\text{C5:}\quad T_{\min} \leq T_s \leq \Theta\tau - T_t \tag{43e}$$

$$\text{C6:}\quad 1 \leq \Theta \leq \Theta_{\max} \tag{43f}$$

Constraint (C1) requires that the minimum rate achieved by DLEO system be greater than the target threshold $C^{\min}_{E3\to S3}$. Constraint (C2) caps the total transmit power of the DLEO earth station at a predefined value $P^{\max}_{E3}$. Constraint (C3) and (C4) imposes the average interference and the instantaneous interference under underlay model at the GEO system as less than a predefined threshold $I^{\max}_{S2}$, respectively. The last Constraint (C5) and (C6) limit the sensing time and the sensing interval.

C. PROPOSED OPTIMAL SOLUTION

Note that problem (43) is highly nonconvex, with the constraints (C1), (C2), (C3) and (C4) that are nonconvex due to coupling among the transmitting power (P^0_{E3}, P^1_{E3}), sensing interval Θ and sensing time T_s. We solve (43) by using a two-dimensional line search method to obtain the optimal Θ and T_s. Therefore, given Θ and T_s, the (43) can be transformed into the following problem.

$$\mathbf{P2}: \underset{P^0_{E3},P^1_{E3}}{\text{maximize}}\ \overline{C_{E3\to S3}}\left(P^0_{E3}, P^1_{E3}\right) \tag{44}$$

$$\text{suject to (C1),}\quad \text{(C2),}\quad \text{(C3),}\quad \text{(C4)} \tag{44a}$$

It can be easily verified that the Hessian matrix of $\overline{C_{E3\to S3}}\left(P^0_{E3}, P^1_{E3}\right)$ is a negative semidefinite matrix. $\overline{C_{E3\to S3}}\left(P^0_{E3}, P^1_{E3}\right)$ is a convex function of P^0_{E3}, P^1_{E3}. Therefore, P2 can be solved by convex optimization techniques. The Lagrangian of (P2) is given by

$$\begin{aligned} &L_{E3\to S3}\left(P^0_{E3}, P^1_{E3}, \mu_0, \mu_1, \kappa, \eta\right) \\ &= \overline{C_{E3\to S3}}\left(P^0_{E3}, P^1_{E3}\right) - \mu_0\left(P^0_{E3} - P^{\max}_{E3}\right) \\ &\quad - \mu_1\left(P^1_{E3} - P^{\max}_{E3}\right) - \kappa\left(\overline{I_{S2}} - I^{\max}_{S2}\right) \\ &\quad - \eta\left(P^1_{E3}G_{S3}\{\beta\} - I^{\max}_{S2}\right) \end{aligned} \tag{45}$$

where $(\mu_0, \mu_1, \kappa, \eta)$ denotes the Lagrange multiplier associated with the constraints in (C2), (C3), (C4). The dual function of (P2) is thus given by

$$\min L_{E3\to S3}\left(P^0_{E3}, P^1_{E3}, \mu_0, \mu_1, \kappa, \eta\right) \tag{46}$$

Since (P2) is a convex optimization problem for which the strong duality holds, the Karush-Kuhn-Tucker (KKT) conditions are both necessary and sufficient for the global optimality of (P2), which are given by

$$\begin{cases} P^{(0)*}_{E3} - P^{\max}_{E3} \leqslant 0 \\ P^{(1)*}_{E3} - P^{\max}_{E3} \leqslant 0 \\ \overline{I_{S2}}(P^{(0)*}_{E3}, P^{(1)*}_{E3}) - I^{\max}_{S2} \leqslant 0 \\ P^{(1)*}_{E3}G_{S3}\{\beta\} - I^{\max}_{S2} \leqslant 0 \end{cases} \tag{47}$$

$$\begin{cases} \mu^*_0\left(P^{(0)*}_{E3} - P^{\max}_{E3}\right) = 0 \\ \mu^*_1\left(P^{(1)*}_{E3} - P^{\max}_{E3}\right) = 0 \\ \kappa^*\left(\overline{I_{S2}}(P^{(0)*}_{E3}, P^{(1)*}_{E3}) - I^{\max}_{S2}\right) = 0 \\ \eta^*\left(P^{(1)*}_{E3}G_{S3}\{\beta\} - I^{\max}_{S2}\right) = 0 \end{cases} \tag{48}$$

$$\begin{cases} \dfrac{\partial}{\partial(P^0_{E3})}\overline{C_{E3\to S3}}\left(P^{(0)*}_{E3}\right) - \mu^*_0 \\ -\dfrac{\kappa^*}{\Theta\tau}((U_{00}v_2 + U_{10}v_3) \times G_{S3}\{\beta\}) = 0 \\ \dfrac{\partial}{\partial(P^1_{E3})}\overline{C_{E3\to S3}}\left(P^{(1)*}_{E3}\right) - \mu^*_1 - \eta^* G_{S3}\{\beta\} \\ -\dfrac{\kappa^*}{\Theta\tau}\left((U_{01}v_2 + U_{11}v_3) \times G_{S3}\{\beta\}\right) = 0 \end{cases} \tag{49}$$

where $\left(P^{(0)*}_{E3}, P^{(1)*}_{E3}\right)$ and $(\mu^*_0, \mu^*_1, \kappa^*, \eta^*)$ denote the optimal primal and dual solutions of (P2), respectively. We then obtain (50) and (51) by solving the equation (49). Firstly, $P^{(1)*}_{E3}$ is given by

$$\begin{aligned} P^{(1)*}_{E3} &= \left[\frac{P_1 + \sqrt{\Delta_1}}{2}\right]^+ \\ P_1 &= -(2N_0 + I_{S3}) \\ &\quad + \frac{\ln 2\,(U_{01}T_{LEO} + U_{11}T_{LEO})}{\mu^*_1\Theta\tau + (\kappa^*(U_{01}v_2 + U_{11}v_3) + \eta^*\Theta\tau)\,G_{S3}\{\beta\}} \\ \Delta_1 &= (P_1)^2 - 4\left(\begin{array}{c}\frac{(U_{01}v_1 + U_{11}v_4)I_{S3}(P_1 + 2N_0 + I_{S3})}{U_{01}T_{LEO} + U_{11}T_{LEO}} \\ -P_1N_0 - N_0^2\end{array}\right) \end{aligned} \tag{50}$$

similarly, $P^{(0)*}_{E3}$ is given by

$$\begin{aligned} P^{(0)*}_{E3} &= \left[\frac{P_0 + \sqrt{\Delta_0}}{2}\right]^+ \\ P_0 &= -(2N_0 + I_{S3}) \\ &\quad + \frac{\ln 2\,(U_{00}v_1 + U_{10}v_3)}{\mu^*_0\Theta\tau + (\kappa^*(U_{00}v_2 + U_{10}v_3)G_{S3}\{\beta\})} \\ \Delta_0 &= (P_0)^2 - 4\left(\begin{array}{c}\frac{U_{00}v_1I_{S3}(P_0 + 2N_0 + I_{S3})}{U_{00}v_1 + U_{10}v_3} \\ -P_0N_0 - N_0^2\end{array}\right) \end{aligned} \tag{51}$$

where $[x]^+$ denotes $\max(x, 0)$. Since there are four equations in (48), we need to discuss 16 cases to obtain the

TABLE 2. Six cases of lagrange multiplier.

Case	μ_0	μ_1	κ	η
1	$P_{E3}^{(0)*}=P_{E3}^{\max}$	$P_{E3}^{(1)*}=P_{E3}^{\max}$	$\kappa^*=0$	$\eta^*=0$
2	$\mu_0^*=0$	$\mu_1^*=0$	$\kappa^*\neq 0$	$\eta^*=0$
3	$P_{E3}^{(0)*}=P_{E3}^{\max}$	$\mu_1^*=0$	$\kappa^*\neq 0$	$\eta^*=0$
4	$\mu_0^*=0$	$P_{E3}^{(1)*}=P_{E3}^{\max}$	$\kappa^*\neq 0$	$\eta^*=0$
5	$P_{E3}^{(0)*}=P_{E3}^{\max}$	$\mu_1^*=0$	$\kappa^*=0$	$P_{E3}^{(1)*}=I_{S2}^{\max}/G_{S3}\{\beta\}$
6	$\mu_0^*=0$	$\mu_1^*=0$	$\kappa^*\neq 0$	$P_{E3}^{(1)*}=I_{S2}^{\max}/G_{S3}\{\beta\}$

TABLE 3. Two-dimensional line search algorithm.

Algorithm The two-dimensional line search algorithm Parameters

C1 Initialization: Set initialization parameters of convex optimization;

Input the minimum rate $C_{E3\to S3}^{\min}$, the total transmit power $P_{E3}^{\max}$, the maximum interference threshold $I_{S2}^{\max}$.

C2 Optimization:

For $1\leq\Theta\leq\Theta_{\max}$

for $T_{\min}\leq T_s\leq\Theta\tau-T_s$ subject to Constraint$(C1)$

1. Initialize $i=1, i\leqslant 6$;

2. Utilizing these parameters in case (i), solve the problem in (45) by equation (50) and (51);

3. If the value satisfy the (47), set $L_{E3\to S3}\{(i)\}\leftarrow(P_{E3}^{(0)*},P_{E3}^{(1)*})$. Otherwise, discard the values;

4. $i=i+1$, go to step 2;

5. Select the minimum value from the set $L_{E3\to S3}$ and obtain the optimal solution:$(P_{E3}^{(0)*},P_{E3}^{(1)*})$.

end

End

C3 Comparison: Compare all $\overline{C_{E3\to S3}}$ and obtain the optimal value $T_s^*=\arg\max_{T_s}\overline{C_{E3\to S3}}(T_s,P_{E3}^{(0)*},P_{E3}^{(1)*})$,

$\Theta^*=\arg\max_{\Theta}C_{E3\to S3}(\Theta,T_s^*,P_{E3}^0,P_{E3}^1)$,

$\overline{C_{E3\to S3}^*}=\overline{C_{E3\to S3}}(\Theta^*,T_s^*,P_{E3}^{(0)*},P_{E3}^{(1)*})$.

optimal value. However, there are 10 cases that are either inconsistent with the actual situation or contradictory, so only six cases need to be considered, which is given in Table 2, that is, the optimal solution can be obtained after six iterations. Therefore, we choose the smallest $L_{E3\to S3}$ as the optimal solution in the set of values satisfying (47), which is denoted as $(P_{E3}^{(0)*},P_{E3}^{(1)*},\mu_0^*,\mu_1^*,\kappa^*,\eta^*)$. It is worth noting that $(P_{E3}^{(0)*},P_{E3}^{(1)*},\mu_0^*,\mu_1^*,\kappa^*,\eta^*)$ satisfying (47) (48) and (49) are uniquely determined since six variables are solutions of six independent equations. Consequently, the algorithm is summarized in Table 3 to solve this problem.

Complexity Analysis: There are three loops in the algorithm: the first and the second loop is used to solve the problem of sensing interval and sensing time allocation, respectively, such that $\Theta_{\max}-$group and $T_{\max}/\tau-$group solutions are obtained; then, in the third loop, we solve P2 through six iterations to obtain the optimal solution $(P_{E3}^{(0)*},P_{E3}^{(1)*})$. Note that there is an operation to get the optimal value after each iteration. By analyzing the algorithm, we can obtain the computational complexity of thye algorithm is $O\left(\left(\Theta_{\max}\left(\frac{T_{\max}}{\tau}(K+1)+1\right)+1\right)\right)$.

IV. NUMERICAL RESULTS

In this section, we evaluate the performance of the proposed design method using computer simulations. The satellite

TABLE 4. Orbital parameters of the GEO and LEO satellites.

Parameters	GEO	LEO
Semimajor axis	42,164.1 km	7378.14 km
Eccentricity	0	0
Inclination angle	0^o	90^o
Right ascension of the ascending node	57^o	277^o
Argument of perigee	0^o	0^o
Time past perigee	$0s$	$0s$

TABLE 5. Simulation parameters.

Parameters	Value
Frequency band f	20GHz(Ka)
Noise temperature of receive antenna T_n	290K
Antenna efficiency η	55%
Antenna diameter of GEO satellite D_G	2.4m
Antenna diameter of GEO station D_{Gu}	0.3m
Transmit power of GEO station P_{E2}	20W
Antenna diameter of LEO satellite D_L	0.1m
Antenna diameter of LEO station D_{Lu}	0.3m
Bandwidth B	25MHz
Sampling frequency of SLEO f_{S1}	10MHz
Length of a slot τ	0.02s
Transmission time T_t	0.01s
Angular velocity of LEO w_0	0.05deg/s
Angle between E2 and E3 $\sigma_{E2\to E3}$	-0.3deg
Angle between E1 and E2 $\sigma_{E1\to E2}$	1.5deg
Minimum rate of LEO system $C_{E3\to S3}^{\min}$	1.2bps/Hz
Maximum transmit power of LEO station $P_{E3}^{\max}$	10W
Maximum interference threshold for GEO $I_{S2}^{\max}$	-130dBw
Maximum sensing interval $\Theta_{\max}$	10
Transmission matrix Δ_{S2}	$\begin{bmatrix}0.7 & 0.3\\ 0.2 & 0.8\end{bmatrix}$

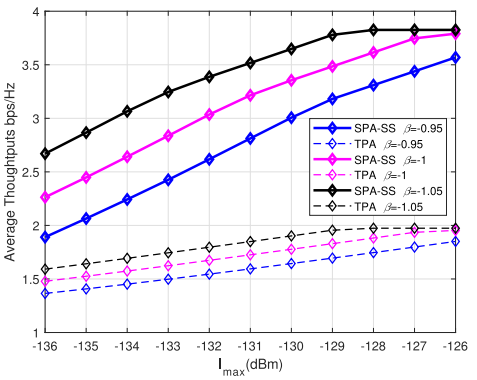

FIGURE 4. Average throughput of the DLEO system versus the interference power constraint at the GEO system.

orbital parameters and simulation parameters for the numerical results are given in Table 4 and Table 5 follow those obtained from [25].

We plot the average throughput and the spectrum sensing interval of the DLEO system versus interference power constraint $I_{S2}^{\max}$. It can be seen from Fig.4 that the average throughput of the DLEO system increases with $I_{S2}^{\max}$, A larger $I_{S2}^{\max}$ implies that the GEO system can tolerate more interferences from the DLEO system, which allows the DLEO system to use a larger transmit power or larger spectrum sensing interval. As shown in Fig.4, the proposed SPA-SS scheme can achieve about higher average throughput of the system than the traditional power allocation scheme (TPA) [26], i.e, the spectrum sensing interval $\Theta=1$. Furthermore, as the angle β between DLEO and GEO

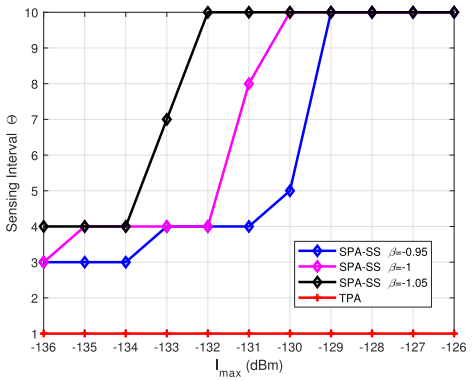

FIGURE 5. Optimal Sensing interval of the DLEO system versus the interference power constraint at the GEO system.

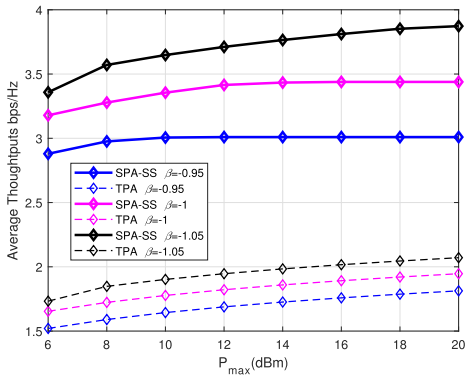

FIGURE 6. Average throughput of the DLEO system versus transmit power constraint at the GEO system.

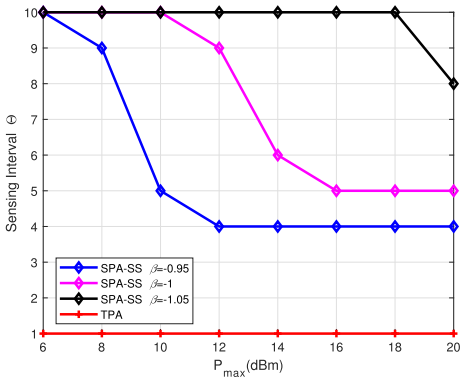

FIGURE 7. Optimal Sensing interval of the DLEO system versus the transmit power constraint at the GEO system.

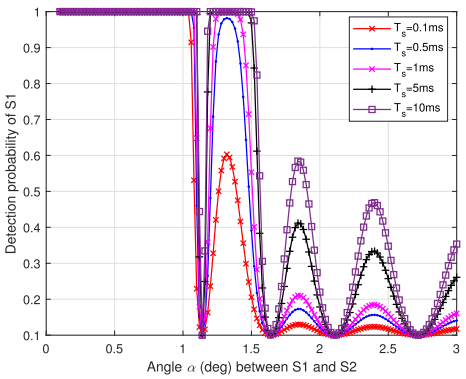

FIGURE 8. The detection probability versus angel α between SLEO and GEO.

satellites increases, the average throughput of DLEO system also increases, which is consistent with the expectation, because the interference between them is reduced.

The average spectrum sensing interval versus the interference power constraint $I_{S2}^{\max}$ is shown in Fig.5. The optimal sensing interval Θ^* increases with the increasing of $I_{S2}^{\max}$ and the angle β. Certainly, a smaller $I_{S2}^{\max}$ implies that the protection requirements of the GEO system is high. However, a bigger value of Θ^* will incur some transmission collisions when the current channel status is idle due to the imperfect sensing. Hence, the LEO system adopts smaller spectrum sensing interval to reduce interference.

Fig.6 shows the trend of the average throughput of the DLEO system versus the transmit power constraint $P_{E3}^{\max}$. In general, the average throughput of the DLEO system increases with increasing $P_{E3}^{\max}$ and the angle β. Another phenomenon is that the curves in Fig.6 become more and more flat because the interference power has greater influence on the average throughput with the increase of $P_{E3}^{\max}$. Fig.7 displays the average spectrum sensing interval versus $P_{E3}^{\max}$. Generally, the optimal sensing interval Θ^* decreases with the increasing of $P_{E3}^{\max}$, and increases with increasing of angle β. However, with the increase of $P_{E3}^{\max}$, the sensing interval will converge to the optimal value under the constraint of $I_{S2}^{\max}$. It should be note that larger transmit power $P_{E3}^{\max}$ will reduce more system throughput when the value of Θ^* is large because a bigger Θ^* will miss more transmission opportunities when the GEO current channel status is busy. Hence, the SLEO system adopts smaller spectrum sensing interval.

Next, we examine the effect of spectrum sensing on the system performance in Fig.[8-9]. Fig.8 shows the detection probability versus the angle α between SLEO and GEO system. It can be seen that the detection probability decreases wavelike with the increase of included angle α, which is in line with the characteristics of satellite beam. Obviously, there are two ways to improve the detection performance. One is in higher SNR, another is to increase the sampling numbers. In other words, when SLEO is at the beam edge, it is necessary to obtain ideal detection performance at the cost of increasing the sensing time. While SLEO is in the center of beam, the signal can be detected in a short time.

Fig.9 shows the average throughput versus sensing time. It is observed that the general tendency of average throughput decreases with an increasing α and spectrum sensing time T_s. The gap among four curves decreases as the sensing time increases, indicating that the detection probabilities of them are gradually approaching. It is worth noting that in the $\alpha = 1.24$ case, there is no inflection point in the curve, in contrast, the optimal sensing times exist in other cases. It is pointed out that the SLEO satellite has higher SNR and better sensing performance in the $\alpha = 1.24$ case, since that increasing the sensing time may only decrease the

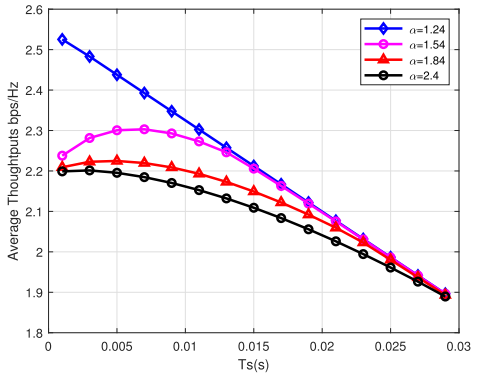

FIGURE 9. Average throughput of the DLEO system versus sensing time of SLEO system.

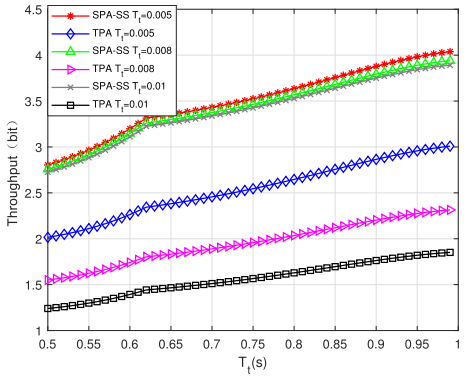

FIGURE 11. Average throughput of the DLEO system versus Transmission time T_t between S1 and E3.

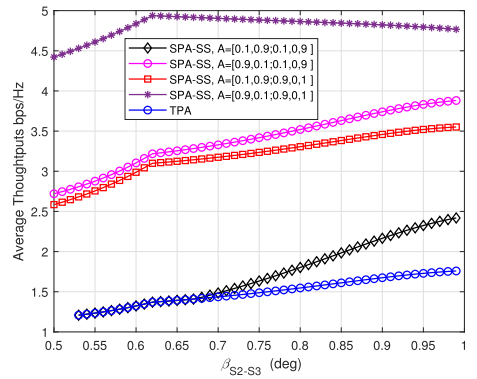

FIGURE 10. Average throughput of the DLEO system versus transmission matrix Δ_{S2} of GEO system when $\sigma_{E2\to E3}$=-0.25.

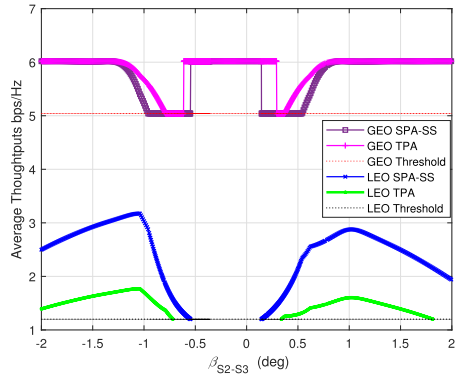

FIGURE 12. Average throughput of the DLEO system versus angel β between S2 and S2 when $\sigma_{E2\to E3} = -0.25$.

transmission time. However, in other cases, increasing the sensing time may upgrade the detection probability, and then improve the throughput of the DLEO system. Therefore, a trade-off between the sensing time and the transmission time is made in order to maximize achievable throughput.

However, compared with the TPA algorithm, the performance gain of SPA-SS algorithm is closely related to both the transmission matrix Δ_{S2} of GEO system and the transmission delay T_t of LEO satellite. One can observe from Fig.10 that the average throughput of the proposed SPA-SS is almost the same as that of APC when $\Delta_{S2} = \begin{bmatrix} 0.1 & 0.9 \\ 0.1 & 0.9 \end{bmatrix}$. This is due to the fact that the LEO system adopts smallest spectrum sensing interval, $\Theta^* = 1$, for protecting the GEO system when it's very busy. Moreover, the SPA-SS algorithm is not sensitive to the frequency of free/busy state changes of GEO system, since it only dependents on the statistical average. Fig.11 also shows that the SPA-SS algorithm can effectively overcome the influence on average throughput caused by transmission delay.

Next, Fig.12 compares the average throughput of the proposed SPA-SS in the whole interference region to that of the TPA. As shown in Fig.12, the average throughput of DLEO system in the proposed SPA-SS is about 30% to 79% higher than that of the TPA. Whereas for GEO system, the average throughput decrease about 16% in the most serious area, but this area is very small and even so, the interference is also above threshold. Another phenomenon is that the throughput of DLEO system turns into 0 when it is very close to the line between the GEO satellite and its earth station. This is due to the interference between the DLEO and GEO system is too large, which makes DLEO system unable to meet its own speed requirements and the tolerable interference of the GEO system at the same time, DLEO system will stop transmitting signals to protect GEO system. Obviously, the non-work region of the proposed SPA-SS is smaller than that of the TPA, which further confirms the superiority of the proposed scheme.

Finally, we plot the time utilization of DLEO system against the angel $\sigma_{E2\to E3}$ in Fig.13. Note that the time utilization is the proportion of available time of DLEO system in the coverage region. In this article, the DLEO satellite coverage region is considered as the plus or minus 2-degree range of E3 station. Furthermore, the Angle Isolation is refer to DLEO system works with fixed power, and will stop working when the interference threshold of the GEO system is triggered, which conforms to relevant ITU-R recommendations. As described in Fig.13, the time utilization of SPA-SS is the highest, with a minimum of 82%, that of TPA is second, which is 60%, and that of Angle Isolation is the last, which is 40%. In addition, the proposed SPA-SS is very effective in the regions of serious interference and the time utilization of that is monotone increasing with $\sigma_{E2\to E3}$. Meanwhile, we can observe that the time utilization rate of the two schemes will

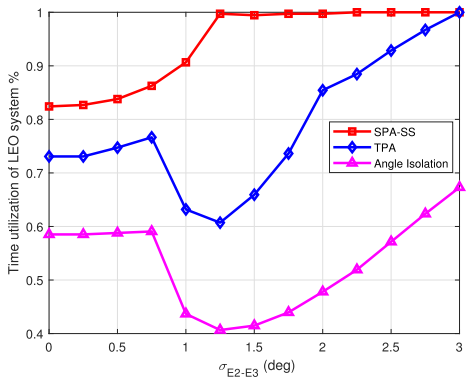

FIGURE 13. Time utilization of the DLEO system versus angel σ between E2 and E3.

up to 100% when the angle $\sigma_{E2\to E3}$ is 3^o, which means that the GEO and LEO system has been able to communicate normally. But for the Angle Isolation algorithm, we need to continue to increase $\sigma_{E2\to E3}$ in order to achieve the normal work of the two systems.

V. CONCLUSION

In this article, we propose a spectrum sharing framework comprised of a GEO satellite and a pair of LEO satellites, where one SLEO is used to sense the status of spectrum occupancy of the GEO, and one DLEO satellite is allowed to access the shared spectrum of the GEO with the aid of the SLEO. Specifically, we analyzed the influence of the high dynamicity of LEO satellite on spectrum sharing. Again, in order to improve the throughput of the DLEO satellite, a SPA-SS algorithm is proposed. Through jointly optimize the spectrum sensing time, the sensing interval and the LEO system transmit power to maximize the throughput of LEO system in interference region. Meanwhile, the objective is optimized subject to the interference constraints of the GEO system the rate constraint, the transmit power constraint of SLEO system. Simulation results showed that the proposed algorithm can well protect the GEO system and achieve higher throughput of the LEO system than the traditional spectrum-sharing scheme. For the future work, as the large-scale constellation of the LEO satellites have been widely deployed, we will extend the proposed algorithm to spectrum sharing between multi-LEO satellites and GEO system under the influence of satellite perturbation.

REFERENCES

[1] *FCC Takes Steps to Facilitate Mobile Broadband and Next Generation Wireless Technologies in Spectrum Above 24 GHz*, FCC, Washington, DC, USA, Jul. 2016.

[2] P. Thompson and B. Evans, "Analysis of interference between terrestrial and satellite systems in the band 17.7 to 19.7 GHz," in *Proc. IEEE Int. Conf. Commun. Workshop (ICCW)*, London, U.K., Jun. 2015, pp. 1669–1674.

[3] J. Hu, G. Li, D. Bian, J. Tang, and S. Shi, "Sensing-based dynamic spectrum sharing in integrated wireless sensor and cognitive satellite terrestrial networks," *Sensors*, vol. 19, no. 23, p. 5290, Dec. 2019.

[4] J. Mitola and G. Q. Maguire, "Cognitive radio: Making software radios more personal," *IEEE Pers. Commun.*, vol. 6, no. 4, pp. 13–18, Aug. 1999.

[5] M. Jia, X. Liu, Z. Yin, Q. Guo, and X. Gu, "Joint cooperative spectrum sensing and spectrum opportunity for satellite cluster communication networks," *Ad Hoc Netw.*, vol. 58, pp. 231–238, Apr. 2017.

[6] Y. Ruan, Y. Li, C.-X. Wang, R. Zhang, and H. Zhang, "Energy efficient power allocation for delay constrained cognitive satellite terrestrial networks under interference constraints," *IEEE Trans. Wireless Commun.*, vol. 18, no. 10, pp. 4957–4969, Oct. 2019.

[7] J. Wang, C. Jiang, H. Zhang, Y. Ren, K.-C. Chen, and L. Hanzo, "Thirty years of machine learning: The road to Pareto-optimal wireless networks," *IEEE Commun. Surveys Tuts.*, early access, Jan. 13, 2020, doi: 10.1109/COMST.2020.2965856.

[8] B. Kim, H. Yu, and S. Noh, "Cognitive interference cancellation with digital channelizer for satellite communication," *Sensors*, vol. 20, no. 2, p. 355, Jan. 2020.

[9] Z. Qin, X. Zhou, L. Zhang, Y. Gao, Y.-C. Liang, and G. Y. Li, "20 years of evolution from cognitive to intelligent communications," *IEEE Trans. Cognit. Commun. Netw.*, vol. 6, no. 1, pp. 6–20, Mar. 2020.

[10] F. F. Digham, M.-S. Alouini, and M. K. Simon, "On the energy detection of unknown signals over fading channels," *IEEE Trans. Commun.*, vol. 55, no. 1, pp. 21–24, Jan. 2007.

[11] Y.-C. Liang, Y. Zeng, E. C. Y. Peh, and A. T. Hoang, "Sensing-throughput tradeoff for cognitive radio networks," *IEEE Trans. Wireless Commun.*, vol. 7, no. 4, pp. 1326–1337, Apr. 2008.

[12] S. Sedighi, A. Taherpour, S. Gazor, and T. Khattab, "Eigenvalue-based multiple antenna spectrum sensing: Higher order moments," *IEEE Trans. Wireless Commun.*, vol. 16, no. 2, pp. 1168–1184, Feb. 2017.

[13] J. Wang, S. Guan, C. Jiang, D. Alanis, Y. Ren, and L. Hanzo, "Network association in machine-learning aided cognitive radar and communication co-design," *IEEE J. Sel. Areas Commun.*, vol. 37, no. 10, pp. 2322–2336, Oct. 2019.

[14] T. Xiong, Y.-D. Yao, Y. Ren, and Z. Li, "Multiband spectrum sensing in cognitive radio networks with secondary user hardware limitation: Random and adaptive spectrum sensing strategies," *IEEE Trans. Wireless Commun.*, vol. 17, no. 5, pp. 3018–3029, May 2018.

[15] T. Liang, K. An, and S. Shi, "Statistical modeling-based deployment issue in cognitive satellite terrestrial networks," *IEEE Wireless Commun. Lett.*, vol. 7, no. 2, pp. 202–205, Apr. 2018.

[16] S. Vassaki, M. I. Poulakis, A. D. Panagopoulos, and P. Constantinou, "Power allocation in cognitive satellite terrestrial networks with QoS constraints," *IEEE Commun. Lett.*, vol. 17, no. 7, pp. 1344–1347, Jul. 2013.

[17] O. Y. Kolawole, S. Vuppala, M. Sellathurai, and T. Ratnarajah, "On the performance of cognitive satellite-terrestrial networks," *IEEE Trans. Cognit. Commun. Netw.*, vol. 3, no. 4, pp. 668–683, Dec. 2017.

[18] X. Yan, K. An, T. Liang, G. Zheng, and Z. Feng, "Effect of imperfect channel estimation on the performance of cognitive satellite terrestrial networks," *IEEE Access*, vol. 7, pp. 126293–126304, 2019.

[19] V. Singh, S. Solanki, and P. K. Upadhyay, "Cognitive relaying cooperation in satellite-terrestrial systems with multiuser diversity," *IEEE Access*, vol. 6, pp. 65539–65547, 2018.

[20] P. Lai, H. Bai, Y. Huang, Z. Chen, and T. Liu, "Performance evaluation of underlay cognitive hybrid satellite–terrestrial relay networks with relay selection scheme," *IET Commun.*, vol. 13, no. 16, pp. 2550–2557, Oct. 2019.

[21] S. Shi, K. An, G. Li, Z. Li, H. Zhu, and G. Zheng, "Optimal power control in cognitive satellite terrestrial networks with imperfect channel state information," *IEEE Wireless Commun. Lett.*, vol. 7, no. 1, pp. 34–37, Feb. 2018.

[22] R. Li, P. Gu, and C. Hua, "Optimal beam power control for co-existing multibeam GEO and LEO satellite system," in *Proc. 11th Int. Conf. Wireless Commun. Signal Process. (WCSP)*, Xi'an, China, Oct. 2019, pp. 1–6.

[23] Y. Su, Y. Liu, Y. Zhou, J. Yuan, H. Cao, and J. Shi, "Broadband LEO satellite communications: Architectures and key technologies," *IEEE Wireless Commun.*, vol. 26, no. 2, pp. 55–61, Apr. 2019.

[24] P. Hajipour, A. Shahzadi, and S. Ghazi-Maghrebi, "Interference management for spectral coexistence in a heterogeneous satellite network," *Int. J. Satell. Commun. Netw.*, vol. 38, no. 3, pp. 229–253, May 2020.

[25] C. Wang, D. Bian, S. Shi, J. Xu, and G. Zhang, "A novel cognitive satellite network with GEO and LEO broadband systems in the downlink case," *IEEE Access*, vol. 6, pp. 25987–26000, 2018.

[26] S. K. Sharma, S. Chatzinotas, and B. Ottersten, "In-line interference mitigation techniques for spectral coexistence of GEO and NGEO satellite," *Int. J. Satell. Commun. Netw.*, vol. 34, no. 1, pp. 11–39, 2016.

[27] C. Zhang, C. Jiang, J. Jin, S. Wu, L. Kuang, and S. Guo, "Spectrum sensing and recognition in satellite systems," *IEEE Trans. Veh. Technol.*, vol. 68, no. 3, pp. 2502–2516, Mar. 2019.

[28] X. Dong, T. Zhang, D. Lu, G. Li, Y. Shen, and J. Ma, "Preserving geo-indistinguishability of the primary user in dynamic spectrum sharing," *IEEE Trans. Veh. Technol.*, vol. 68, no. 9, pp. 8881–8892, Sep. 2019.
[29] F. Vatalaro, G. E. Corazza, C. Caini, and C. Ferrarelli, "Analysis of LEO, MEO, and GEO global mobile satellite systems in the presence of interference and fading," *IEEE J. Sel. Areas Commun.*, vol. 13, no. 2, pp. 291–300, Feb. 1995.
[30] H. Wang, C. Wang, J. Yuan, Y. Zhao, R. Ding, and W. Wang, "Coexistence downlink interference analysis between LEO system and GEO system in ka band," in *Proc. IEEE/CIC Int. Conf. Commun. China (ICCC)*, Beijing, China, Aug. 2018, pp. 465–469.
[31] M. Höyhtyä, A. Mämmelä, X. Chen, A. Hulkkonen, J. Janhunen, J.-C. Dunat, and J. Gardey, "Database-assisted spectrum sharing in satellite communications: A survey," *IEEE Access*, vol. 5, pp. 25322–25341, 2017.
[32] C. Zhang, C. Jiang, L. Kuang, J. Jin, Y. He, and Z. Han, "Spatial spectrum sharing for satellite and terrestrial communication networks," *IEEE Trans. Aerosp. Electron. Syst.*, vol. 55, no. 3, pp. 1075–1089, Jun. 2019.
[33] X. Xing, T. Jing, W. Cheng, Y. Huo, and X. Cheng, "Spectrum prediction in cognitive radio networks," *IEEE Wireless Commun.*, vol. 20, no. 2, pp. 90–96, Apr. 2013.
[34] J. Sun, L. Shen, G. Ding, R. Li, and Q. Wu, "Predictability analysis of spectrum state evolution: Performance bounds and real-world data analytics," *IEEE Access*, vol. 5, pp. 22760–22774, 2017.
[35] H. Eltom, S. Kandeepan, Y.-C. Liang, and R. J. Evans, "Cooperative soft fusion for HMM-based spectrum occupancy prediction," *IEEE Commun. Lett.*, vol. 22, no. 10, pp. 2144–2147, Oct. 2018.
[36] L. Li and A. Ghasemi, "IoT-enabled machine learning for an algorithmic spectrum decision process," *IEEE Internet Things J.*, vol. 6, no. 2, pp. 1911–1919, Apr. 2019.
[37] X. Xing, T. Jing, H. Li, Y. Huo, X. Cheng, and T. Znati, "Optimal spectrum sensing interval in cognitive radio networks," *IEEE Trans. Parallel Distrib. Syst.*, vol. 25, no. 9, pp. 2408–2417, Sep. 2014.
[38] B. Liu, Z. Li, J. Si, and F. Zhou, "Optimal sensing interval in cognitive radio networks with imperfect spectrum sensing," *IET Commun.*, vol. 10, no. 2, pp. 189–198, Jan. 2016.
[39] I. A. M. Balapuwaduge, F. Y. Li, and V. Pla, "System times and channel availability for secondary transmissions in CRNs: A dependability-theory-based analysis," *IEEE Trans. Veh. Technol.*, vol. 10, no. 2, pp. 189–198, Jan. 2016.
[40] X. Li and J. Wang, "Elastically reliable video transport protocol over lossy satellite links," *IEEE J. Sel. Areas Commun.*, vol. 36, no. 5, pp. 1097–1108, May 2018.
[41] E. Kaplan and C. Hegarty, "Fundamentals of satellite navigation," in *Understanding GPS: Principles and Applications*, 2nd ed. London, U.K.: Artech House, 2005, ch. 2, sec. 3, pp. 34–43.
[42] M. A. Diaz, N. Courville, C. Mosquera, G. Liva, and G. E. Corazza, "Non-linear interference mitigation for broadband multimedia satellite systems," in *Proc. Int. Workshop Satell. Space Commun. (IWSSC)*, Sep. 2007, pp. 61–65.

YUNFENG WANG received the B.E. degree in communication engineering from Shandong Normal University, Shandong, China, in 2009. He is currently pursuing the Ph.D. degree in satellite communication with the Satellite and Mobile Communication Section, Nanjing University of Posts and Telecommunications.

His research interests include spectrum sensing, cooperative communications, spectrum interference, and game theory.

XIAOJIN DING (Member, IEEE) received the Ph.D. degree in information and communication engineering from the National Mobile Communication Research Laboratory, Southeast University (SEU), Nanjing, China.

He is currently a Lecturer with the Nanjing University of Posts and Telecommunications (NUPT), Nanjing. His research interests include space information networks, cooperative communications, and physical-layer security.

GENGXIN ZHANG (Member, IEEE) received the bachelor's, master's, and Ph.D. degrees from the Department of Radio Communication Engineering, Nanjing Institute of Communication Engineering, Nanjing, China, in 1987, 1990, and 1994, respectively.

He is currently a Professor with the Nanjing University of Posts and Telecommunications (NUPT), Nanjing. His research interests include satellite communications, deep space communications, and space information networks. He is also heading several projects in these areas.